NUMERICAL SIMULATION OF WATERJET EXCAVATION IN SOFT ROCK

Yuichi YUMOTO

1. INTRODUCTION

We gain variable things by using nature, for example, fossil fuels, natural gas and building underground constructions. These approach need to know the characteristic of soft rock. Methane hydrate is a consolidated methane gas, and draw attention as new energy source. The layer contained Methane hydrate is a kind of soft rock. Recently, Waterjet technology is watched as one of the drilling method. The characteristics of Waterjet are a low drilling cost because of using only water, a safety because of not striking a spark, and capable of miniaturization and weight saving. However, since the performance of waterjet technologies depends on many parameters, many experiments are required to develop a waterjet technology. Thus, numerical simulation of waterjet excavation in soft rock can help decreasing the development cost. Because both solid and liquid are greatly deformed in waterjet excavation, it is difficult to model this problem by using a finite element method.

The smoothed particle hydrodynamics (SPH) is a fully Lagrangian technique in which the numerical solution is achieved without grid. An advantage of the SPH is the relative ease with which new physics may be incorporated into the formulation. It is also straightforward to allow boundaries to move or deform and to model the interaction between fluid and solid, and to extend to three dimensions. There have been some studies on the SPH simulation for waterjet drilling, but there is no research on soft rock.

Shoji(2010) used SPH method and conducted waterjet and rock modeling, and described rock excavation behavior. However, it remained the problem of not ejecting fracture rock particles. Also, the case of methane hydrate drilling, its simulation code cannot use because of not considering pore water pressure.

In this study, I aimed to develop a waterjet drilling simulation method which Shoji(2010) developed for soft rock and saturated rock based on real excavation mechanism for rock. The contents of this study are as follows:

1) Improvement of the fracture particles treatment which is an outstanding issue in Shoji's research.
2) Modeling of rock contained pore water, and two kind of filled water particles pattern, then comparing drilling behavior between the saturated rock and the dry rock.
3) Comparison of the simulation result on the saturated rock excavation with the dry rock excavation.
4) Comparison of the simulation results on waterjet saturated rock excavation based on two failure criterions with the experimental results.

2. MODELING BY SPH
2.1 Basic ideas of SPH

For a given function $\phi(\boldsymbol{r})$, the expression of particle approximation by using kernel function $(\langle\phi(\boldsymbol{r})\rangle)$ is defined as

$$\langle\phi(\boldsymbol{r})\rangle = \int_{\Omega}\phi(\boldsymbol{r}')W(\boldsymbol{r}-\boldsymbol{r}',h)d\boldsymbol{r}', \qquad (1)$$

where Ω is the volume of the object; $\boldsymbol{r}$ is the current position vectors; h is called smoothing length that controls the influence domain, and $W(\boldsymbol{r}-\boldsymbol{r}',h)$ is kernel function (Fig. 1), which must satisfy the following three properties:

$$\lim_{h\to 0}W(\boldsymbol{r}-\boldsymbol{r}',h)=\delta(\boldsymbol{r}-\boldsymbol{r}'), \qquad (2)$$

$$\int_{\Omega}W(\boldsymbol{r}-\boldsymbol{r}',h)d\boldsymbol{r}'=1, \qquad (3)$$

$$W(\boldsymbol{r}-\boldsymbol{r}',h)=0 \quad \text{for} \quad |\boldsymbol{r}-\boldsymbol{r}'|\geq h. \qquad (4)$$

In this study, the cubic spline interpolation function was used as kernel function.

In the SPH method, the calculation domain is represented by N points (particles), which carry mass and field variable information such as density, stress, etc. Accordingly, the continuous integral representation for $\phi(\boldsymbol{r})$ is approximated, and the particle approximation ϕ_i at particle i can be written as

$$\phi_i = \sum_{j}^{N}m_j\frac{\phi_j}{\rho_j}W_{ij}, \qquad (5)$$

where m_j is the mass and ρ_j is the density of the jth particle, and $W_{ij}=W(\boldsymbol{r}_i-\boldsymbol{r}_j,h)$.

Following the same argument, the particle approximation for the spatial derivative of the function at particle i is

$$\left(\frac{\partial\phi}{\partial x^{\alpha}}\right)_i = \sum_{j}^{N}m_j\frac{\phi_j}{\rho_j}\frac{\partial W_{ij}}{\partial x^{\alpha}}, \qquad (6)$$

where x^{α} is the orthogonal coordinate axis, and the Greek superscripts denote the spatial
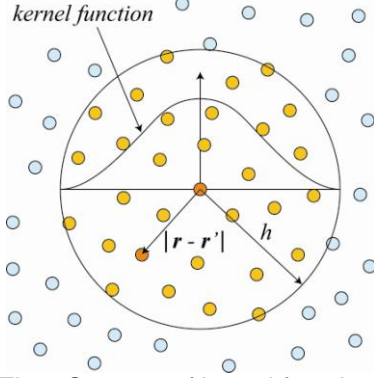
coordinate directions.

Fig.1 Concept of kernel function.

2.2 Modeling of waterjet

Waterjet is assumed to be a viscous fluid with weak compressibility. The governing equations are the equations of continuity, motion and state, as given by

$$\frac{D\rho}{Dt} = -\rho \frac{\partial v^\alpha}{\partial x^\alpha}, \tag{7}$$

$$\frac{Dv^\alpha}{Dt} = \frac{1}{\rho} \frac{\partial \sigma^{\alpha\beta}}{\partial x^\beta} + f^\alpha, \tag{8}$$

$$P = B\left[\left(\frac{\rho}{\rho_0}\right)^\gamma - 1\right], \tag{9}$$

where t is time, v^α is the velocity vector, $\sigma^{\alpha\beta}$ is the total stress tensor, f^α is the external force, P is pressure, ρ_0 is initial density, $\gamma = 7$ and B is a constant related to the bulk modulus of elasticity of the fluid.

The stress tensor consists of two parts: pressure term and viscous term,

$$\sigma^{\alpha\beta} = -P\delta^{\alpha\beta} + \mu T^{\alpha\beta}, \tag{10}$$

where μ is the dynamic viscosity and $T^{\alpha\beta}$ is the shear strain rate.

Converting and applying the SPH particle approximation to the Eqs. (7) and (8), the equations of continuity and motion on particle i in the SPH formulation are

$$\frac{D\rho_i}{Dt} = \sum_j^N m_j \left(v_i^\alpha - v_j^\alpha\right) \frac{\partial W_{ij}}{\partial x^\alpha}, \tag{11}$$

$$\frac{Dv^\alpha}{Dt} = \sum_j^N m_j \left(\frac{\sigma_i^{\alpha\beta}}{\rho_i^2} + \frac{\sigma_j^{\alpha\beta}}{\rho_j^2}\right) \frac{\partial W_{ij}}{\partial x^\beta} + f_i^\alpha, \tag{12}$$

2.3 Modeling of saturated rock materials

Modeling the behavior of rock using the SPH method is similar to that of water. Since rock is assumed to be elastic, Hooke's law is used for the equation of state,

$$P = K\eta = K\left(\frac{\rho}{\rho_0} - 1\right), \tag{13}$$

where K is bulk modulus, and η is the volumetric strain.

Eqs. (12) and (13) are also used to estimate the density and motion of rock particles. However, the stress tensor does not include the viscosity term, but includes the deviatoric stress,

$$\sigma^{\alpha\beta} = -P\delta^{\alpha\beta} + s^{\alpha\beta}. \tag{14}$$

The deviatoric stress $s^{\alpha\beta}$ can be estimated using the Jaumann stress rate,

$$\dot{s}^{\alpha\beta} = 2G\left(\dot{\varepsilon}^{\alpha\beta} - \frac{1}{3}\delta^{\alpha\beta}\dot{\varepsilon}^{\gamma\gamma}\right) + s^{\alpha\gamma}\omega^{\beta\gamma} + s^{\gamma\beta}\omega^{\alpha\gamma}, \tag{15}$$

where G is the shear modulus, $\dot{s}^{\alpha\beta}$ is the deviatoric stress rate, $\dot{\varepsilon}^{\alpha\beta}$ is the strain rate tensor and $\omega^{\alpha\beta}$ is the rotation tensor.

The pore pressure P_{pore} is important to model the saturated rock, and given by,

$$P_{pore} = -\sum_{a=1}^N m_a \frac{p_a}{\rho_i \rho_a} \frac{\partial W_{ia}}{\partial x^\beta} \tag{16}$$

where a is the number of water particles. The formula of pore pressure is substituted into the momentum equation of rock.

2.4 Artificial viscosity

To prevent unphysical penetration of particles, an artificial viscosity has been introduced to the pressure term in the equation of motion. Artificial viscosity Π_{ij} is defined as

$$\Pi_{ij} = \begin{cases} \dfrac{-\alpha \bar{c}_{ij}\lambda_{ij} + \beta\lambda_{ij}^2}{\bar{\rho}_{ij}} & v_{ij} \cdot r_{ij} < 0 \\ 0 & v_{ij} \cdot r_{ij} \geq 0 \end{cases}, \tag{16}$$

where

$$\lambda_{ij} = \frac{\bar{h}_{ij} v_{ij} \cdot r_{ij}}{r_{ij}^2 + \varphi^2}, \tag{17}$$

$$v_{ij} = v_i - v_j, \quad r_{ij} = r_i - r_j. \tag{18}$$

In the above equations, v and c represent the particle velocity vector and the speed of sound. The factor $\phi = 0.1h$ is inserted to prevent numerical divergences when two particles are approaching each other. Bars denote the mean value, and α and β are constants. In this study, there values were set to $\alpha = 0.01$ and $\beta = 0$ for water and $\alpha = 2.5$ and $\beta = 2.5$ for rock.

3. EXCAVATION CONDITION OF SOFT ROCK

3.1 Modified of fracture particles behavior

To show more adequate drilling, a repulsive force using boundary condition added in the fracture particles and non-fracture particles.

The formula of a repulsive force f is,

$$f = \begin{cases} D\left[\left(\dfrac{r_0}{r_{ij}}\right)^{q_1} - \left(\dfrac{r_0}{r_{ij}}\right)^{q_2}\right]\dfrac{\mathbf{r}_{ij}}{r_{ij}^2} & r_{ij} \leq r_0 \\ 0 & r_{ij} < r_0 \end{cases}, \quad (19)$$

r_0 is a beginning distance of particle i and j, $q_1 = 4$ and $q_2 = 2$ in this study.

3.2 Pore water setting pattern

In this study, I approached two pore water setting patterns. Figs and show the layout of water particles in body-centered cubic lattice and in checkered pattern. Fig 2 shows the setting pattern. Water particles in body-centered cubic lattice are twice as much as that in checkered pattern. This approach conducted to verify the water density influence.

(a)   (b)
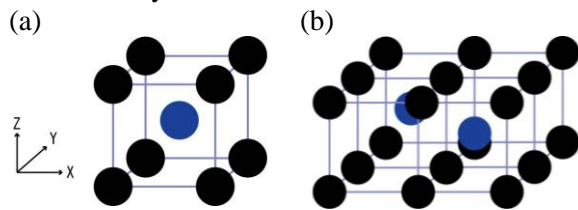
Fig. 2 Pore water setting pattern, body-centered cubic lattice(a) and checkered pattern(b).

3.3 Failure criterion

Shoji(2010) suggested five failure criterions, and evaluated two criterion to explain adequate rock fracture, criterion of the critical strain and critical travel distance. In this study, for these two criterions, I verified which criterions are more adequate. Fig. 3 shows the two criterions.
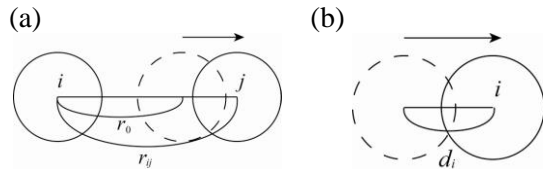
(a)   (b)

Fig. 3 Failure criterions of critical strain(a) and travel distance(b).

3.4 Comparison with experimental

To verify the adequacy of saturated soft rock, an experiment of waterjet excavation was conducted. Kimachi sandstone which is a kind of the soft rock was used as specimen. Table. 1 shows the parameter of Kimachi sandstone. To saturate Kimachi sandstone, it was kept into water for two days. For comparing, waterjet excavation was conducted to the dry Kimachi sandstone. The nozzle diameter was 1 mm, the driving pressure was 30 MPa (velocity = 250 m/s) and the standoff distance was 5.0 mm.

Table. 1 Rock properties of Kimachi sandstone.

Young's modulus, E [GPa]	7.7
Poisson's ratio, ν [−]	0.2
Density, ρ [kg/m^3]	2000

4. RESULTS AND DISCUSSION

4.1 Influence of improvement of fracture particles

It appears that the fracture particles added a force are ejected out of borehole compared with Shoji's(2010). Consequently, adding repulsive force has proved to become better results.

4.2 Influence of pore water setting pattern

Figs. 4 and 5 show the results for the water particles in body-centered cubic lattice and in checkered pattern in critical strain criterion. The excavated ratio is 0.698 % at body-centered cubic lattice and 0.479 % at checkered pattern. It is considered that if the number of pore water particles is larger, the pore pressure is larger, and then the effective stress becomes small, consequently the rock bonding force becomes small.

4.3 Influence of the failure criterion

Figs. 6 and 7 show the results when failure criterion is a critical strain and a travel distance, respectively. Comparing the shape of borehole, the criterion of critical strain has the columnar shape, on the other hand, the criterion of critical travel distance has the bowl shape.

4.4 Verifying Numerical and experimental results

Fig. 8 shows the experimental results of borehole of dry and saturated Kimachi sandstone. Observing the boreholes, the borehole entrance of saturated rock is larger than that of dry rock, and the bottom of the borehole is the shape of column.

As the failure criterion, the critical strain criterion was used, because its borehole is similar to experimental result. Figs. 9 and 10 show the numerical results of borehole of dry and saturated rock. Comparing the entrance of borehole, the saturated rock is larger than dry rock. It is similar to experimental results.
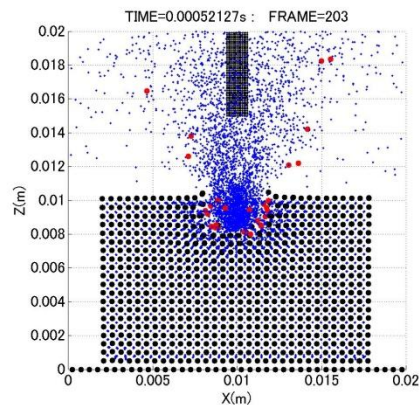

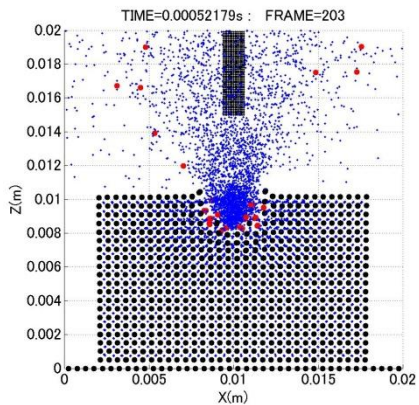Fig. 4 Result for body-centered cubic lattice.
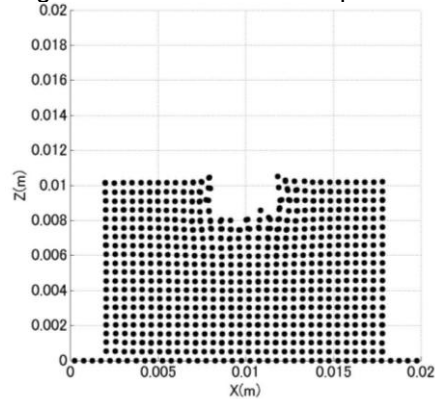
Fig. 5 Result for checkered pattern.

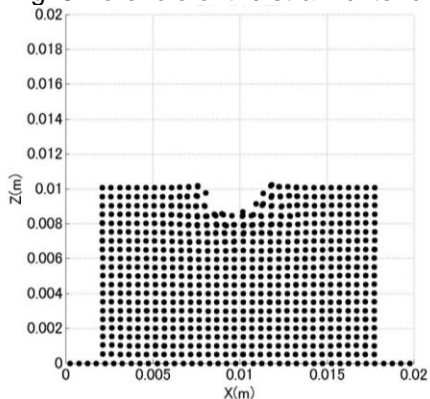Fig. 6 Borehole of the strain criterion.

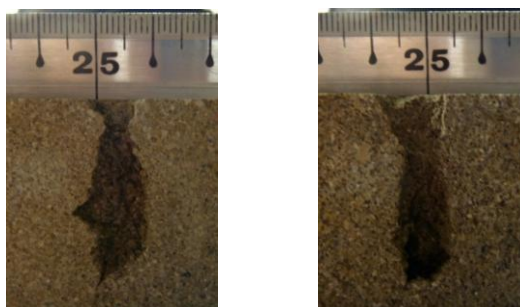Fig. 7 Borehole of the travel distance criterion.

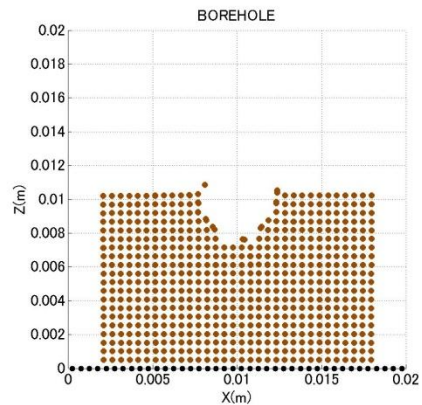Fig. 8 Cross section of borehole of Kimachi dry(left) and saturated(right) sandstones.

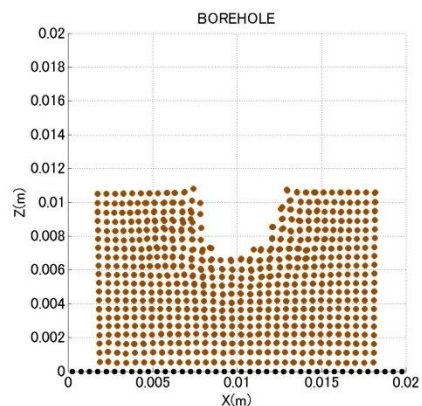Fig. 9 Borehole of the dry rock modeling Kimachi sandstone.

Fig. 10 Borehole of the saturated rock modeling Kimachi sandstone.

5. CONCLUSIONS

Main results obtained in this study can be summarized as follows:
1) Adding a repulsing force for fractured rock particles showed excretory effect from borehole.
2) To model a saturated soft rock, the pore pressure was used between pore water particles and rock particles.
3) The difference of number of pore water particles gave the performance of drilling.
4) From results of experiment, the strain criterion is better than the traveling distance criterion.
5) Comparing experimental and numerical results, it is similar to excavation behavior about saturated rock.

REFERENCES

[1] M. G. Gesteira *et al*, SPHysics
[2] Shoji, 2010, Numerical simulation of waterjet excavation in rock using SPH method, Tohoku Univ. Master thesis.

iv